Werk

Jahr: 1975
Kollektion: fid.geo
Signatur: 8 Z NAT 2148:41
Digitalisiert: Niedersächsische Staats- und Universitätsbibliothek Göttingen
Werk Id: PPN1015067948_0041
PURL: http://resolver.sub.uni-goettingen.de/purl?PPN1015067948_0041

LOG Id: LOG_0019
LOG Titel: Electromagnetic induction in three-dimensional structures
LOG Typ: article

Übergeordnetes Werk

Werk Id: PPN1015067948
PURL: http://resolver.sub.uni-goettingen.de/purl?PPN1015067948
OPAC: http://opac.sub.uni-goettingen.de/DB=1/PPN?PPN=1015067948

Contact

Niedersächsische Staats- und Universitätsbibliothek Göttingen
Georg-August-Universität Göttingen
Platz der Göttinger Sieben 1
37073 Göttingen
Germany
Email: gdz@sub.uni-goettingen.de

J. Geophys. 41, 85–109, 1975

Electromagnetic Induction in Three-Dimensional Structures

P. Weidelt

Institut für Geophysik der Universität, Göttingen

Received August 14, 1974

Abstract. The treatment of electromagnetic induction in three-dimensional structures is simplified by converting Maxwell's equations to a linear inhomogeneous vector integral equation over the domain where the electrical conductivity deviates from a horizontally layered structure. An algorithm for the calculation of the (tensor) kernel is given. The integral equation is solved either by an iterative method or by matrix inversion. In an application the complete electromagnetic surface field of a simple conductivity anomaly and induction arrow maps are given. The gradual transition from three to two dimensions is investigated for a particular model.

Key words: Electromagnetic Induction — Electrical Conductivity — Conductivity Anomalies.

1. Introduction

Numerical solutions of the three-dimensional modelling problem of electromagnetic induction are only scarcely encountered in the current literature (e.g. Jones and Pascoe, 1972; Lines and Jones, 1973). This is not due to mathematical difficulties, but results from the fact that the usual reduction of Maxwell's equations to finite differences, including into the domain under consideration the air half-space, requires large computer storage and is time consuming as well.

A reduction of computer time and storage is achieved by applying surface and volume integral techniques based on Green's tensor. Consider for example an anomalous three-dimensional conductivity structure of finite extent embedded in a normal conductivity structure consisting of a horizontally stratified half-space. Then given an external source field, Maxwell's equations have to be solved under the condition of vanishing anomalous field at infinity. At least three approaches to a numerical solution of this problem are possible. Approach A is to choose a basic domain (including the air layer) as large as possible and to solve within this domain Maxwell's equations by finite differences, subject either to the now only approximate boundary condition of zero anomalous field or to a more refined impedance boundary condition (Fig. 1, top). This is the approach

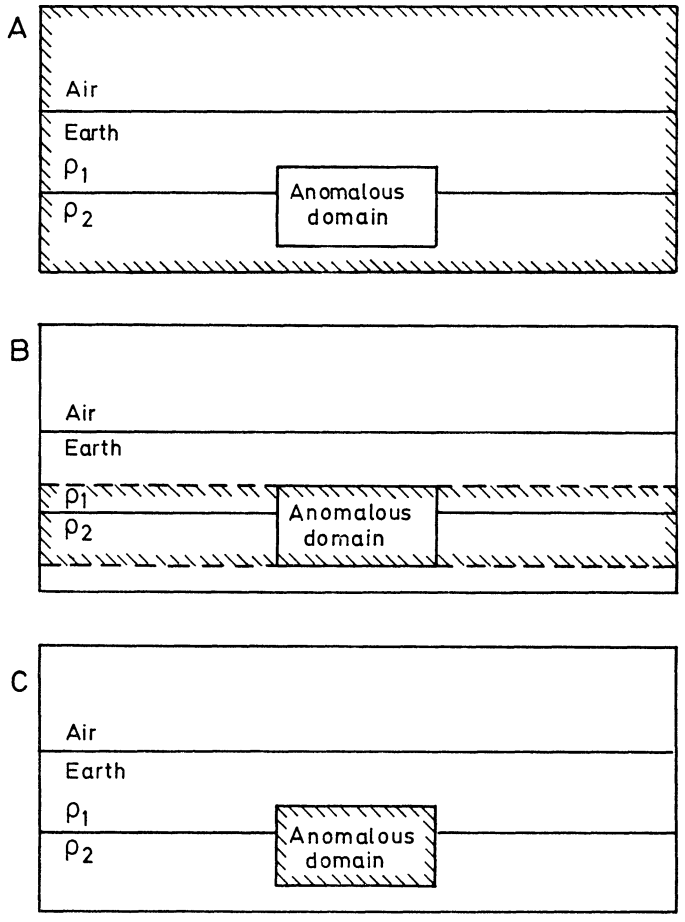

Fig. 1. The three different choices of a basic domain (boundary hatched) for model calculations

of Jones and co-workers. A first reduction of the basic domain is achieved by considering only the anomalous slab which contains the conductivity anomaly (Fig. 1, centre). Within this slab, Maxwell's equations are solved by finite differences as before, but now all field values outside the anomalous slab are expressed by a surface integral in terms of the tangential component of the anomalous electric field at the horizontal boundaries of the slab. At the vertical boundaries of the anomalous slab approximate boundary conditions analogous to those of approach A are applied. This is approach B. A modified version of it for two dimensions is used by Schmucker (1971). In approach C the basic domain is reduced

still further by deriving from Maxwell's equations by a Green's tensor an integral equation for the electric field involving volume integrals only over the anomalous field vector within the anomalous domain (Fig. 1, bottom). The boundary conditions are incorporated in the kernel of the integral equation, and hence are satisfied automatically by the solution. This method has been applied in two dimensions by Hohmann (1972) and has been formulated in three dimensions by Raiche (1974).

From approach A to C the gradual reduction of the basic domain must be paid by increasing expenses for calculating the required kernels. Approach C is of particular advantage if the anomalous domain is small. If the domain extends appreciably in horizontal direction (e.g. different conductivities at the left and the right of the anomalous slab), approach B is appropriate. Approach A can be avoided in any case.

This paper presents a short outline of approach B and a detailed description of approach C, thereby reformulating the method of Raiche (1974) in a slightly different way. The basic equations are stated in Sec. 2, general formulae for Green's tensor for an earth with an arbitrary number of layers are given in Sec. 3, and a few numerical problems encountered in applying approach C are treated in Sec. 4. The final Sec. 5 presents some results.

2. Green's Tensor Approaches to the Modelling Problem

2.1. Definitions, Basic Equations

$\boldsymbol{r}$ denotes the position vector and x, y, z (z positive downwards) are cartesian coordinates, which for the sake of convenience are sometimes also denoted by x_1, x_2, x_3. Let the conductor with conductivity $\sigma(\boldsymbol{r})$ occupy the half-space $z > 0$. Neglecting the displacement current, assuming vacuum permeability and a harmonic time factor $e^{i\omega t}$ throughout, the complex amplitudes $\boldsymbol{E}$ and $\boldsymbol{H}$ of the electric and magnetic field vector are related by

$$\operatorname{curl} \boldsymbol{H}(\boldsymbol{r}) = \sigma(\boldsymbol{r})\, \boldsymbol{E}(\boldsymbol{r}) + \boldsymbol{j}_e(\boldsymbol{r}), \tag{2.1}$$

$$\operatorname{curl} \boldsymbol{E}(\boldsymbol{r}) = -i\omega\mu_0 \boldsymbol{H}(\boldsymbol{r}), \tag{2.2}$$

or combined

$$\operatorname{curl}^2 \boldsymbol{E}(\boldsymbol{r}) + k^2(\boldsymbol{r})\, \boldsymbol{E}(\boldsymbol{r}) = -i\omega\mu_0 \boldsymbol{j}_e(\boldsymbol{r}), \tag{2.3}$$

SI units being used. $\boldsymbol{j}_e(\boldsymbol{r})$ is the current density of the external source field, $\operatorname{curl}^2 = \operatorname{curl} \operatorname{curl}$, and

$$k^2(\boldsymbol{r}) = i\omega\mu_0\sigma(\boldsymbol{r}). \tag{2.4}$$

Split $\sigma(\boldsymbol{r})$ into a normal and anomalous part, the former consisting of a set of horizontal uniform layers. (For simplicity, within the earth all layer conductivities are assumed to be non-zero.) Hence,

$$\sigma = \sigma_n + \sigma_a,\ k^2 = k_n^2 + k_a^2,\ \boldsymbol{E} = \boldsymbol{E}_n + \boldsymbol{E}_a, \tag{2.5}$$

$\boldsymbol{E}_n$ being defined as the solution of

$$\text{curl}\ {}^2\boldsymbol{E}_n(\boldsymbol{r}) + k_n^2(\boldsymbol{r})\,\boldsymbol{E}_n(\boldsymbol{r}) = -\,i\omega\mu_0\,\boldsymbol{j}_e(\boldsymbol{r}), \tag{2.6}$$

vanishing for $z \to \infty$. Methods for the computation of $\boldsymbol{E}_n$ are well-known (e.g. Schmucker, 1970; Weaver, 1970).

2.2. The Volume Integral Method (Approach C)

From (2.3), (2.5), and (2.6) follows

$$\text{curl}\ {}^2\boldsymbol{E}_a(\boldsymbol{r}) + k_n^2(\boldsymbol{r})\,\boldsymbol{E}_a(\boldsymbol{r}) = -\,k_a^2(\boldsymbol{r})\boldsymbol{E}(\boldsymbol{r}). \tag{2.7}$$

Let $\boldsymbol{G}_i(\boldsymbol{r}_0|\boldsymbol{r})$, $i = 1,2,3$, be the solution of

$$\text{curl}\ {}^2\boldsymbol{G}_i(\boldsymbol{r}_0|\boldsymbol{r}) + k_n^2(\boldsymbol{r})\,\boldsymbol{G}_i(\boldsymbol{r}_0|\boldsymbol{r}) = \hat{\boldsymbol{x}}_i\,\delta(\boldsymbol{r}-\boldsymbol{r}_0), \tag{2.8}$$

vanishing at infinity. In (2.8) and in the sequel, $\hat{}$ denotes a unit vector. Multiply (2.8) by $\boldsymbol{E}_a(\boldsymbol{r})$ and (2.7) by $\boldsymbol{G}_i(\boldsymbol{r}_0|\boldsymbol{r})$ and integrate the difference with respect to $\boldsymbol{r}$ over the whole space. Green's vector theorem (e.g. Morse and Feshbach, 1953, p. 1768)

$$\begin{aligned}&\int\{\boldsymbol{U}\cdot\text{curl}\ {}^2\boldsymbol{V} - \boldsymbol{V}\cdot\text{curl}\ {}^2\boldsymbol{U}\}d\tau\\ &= \oint\{\hat{\boldsymbol{n}}\times\boldsymbol{V})\cdot\text{curl}\ \boldsymbol{U} - (\hat{\boldsymbol{n}}\times\boldsymbol{U})\cdot\text{curl}\ \boldsymbol{V}\}dA,\end{aligned} \tag{2.9}$$

where $d\tau$ is a volume element, dA a surface element, and $\hat{\boldsymbol{n}}$ the outward normal vector, yields

$$E_{ai}(\boldsymbol{r}_0) = -\int k_a^2\,\boldsymbol{G}_i(\boldsymbol{r}_0|\boldsymbol{r})\cdot\boldsymbol{E}(\boldsymbol{r})d\tau, \quad i = 1,2,3, \tag{2.10}$$

since $\boldsymbol{E}_a$ and $\boldsymbol{G}_i$ vanish at infinity. After combining all three components and introducing $\boldsymbol{E}$ instead of $\boldsymbol{E}_a$, the vector integral equation

$$\boldsymbol{E}(\boldsymbol{r}_0) = \boldsymbol{E}_n(\boldsymbol{r}_0) - \int k_a^2(\boldsymbol{r})\,\mathfrak{G}(\boldsymbol{r}_0|\boldsymbol{r})\cdot\boldsymbol{E}(\boldsymbol{r})d\tau \tag{2.11}$$

is obtained. Here $\mathfrak{G}$ is the Green's tensor (using dyadic notation)

$$\mathfrak{G}(\boldsymbol{r}_0|\boldsymbol{r}) = \sum_{i=1}^{3} \hat{\boldsymbol{x}}_i \boldsymbol{G}_i(\boldsymbol{r}_0|\boldsymbol{r}) = \sum_{i,\,j=1}^{3} G_{ij}(\boldsymbol{r}_0|\boldsymbol{r})\, \hat{\boldsymbol{x}}_i\, \hat{\boldsymbol{x}}_j. \tag{2.12}$$

The tensor elements G_{ij} admit a simple physical interpretation: $G_{ij}(\boldsymbol{r}_0|\boldsymbol{r})$ is the j-th electric field component of an oscillating electric dipole of unit moment pointing in x_i-direction, placed in the *normal* conductivity structure at $\boldsymbol{r}_0$; the point of observation is $\boldsymbol{r}$. Note that the first index and argument refer to the source, the second index and argument to the observer. Because of the fundamental reciprocity in electromagnetism, observer and source parameters are interchangeable, i.e.

$$G_{ij}(\boldsymbol{r}_0|\boldsymbol{r}) = G_{ji}(\boldsymbol{r}|\boldsymbol{r}_0). \tag{2.13}$$

For a proof replace in (2.8) $\boldsymbol{r}$ by $\boldsymbol{r}'$, write an analogous equation for $\boldsymbol{G}_j(\boldsymbol{r}|\boldsymbol{r}')$, multiply cross-wise by $\boldsymbol{G}_j$ and $\boldsymbol{G}_i$, integrate the difference with respect to $\boldsymbol{r}'$ over the whole space, and obtain (2.13) on using (2.9). Due to (2.13), (2.11) is alternatively written

$$\boldsymbol{E}(\boldsymbol{r}_0) = \boldsymbol{E}_n(\boldsymbol{r}_0) - \int k_a^2(\boldsymbol{r})\, \boldsymbol{E}(\boldsymbol{r}) \cdot \mathfrak{G}(\boldsymbol{r}|\boldsymbol{r}_0) d\tau. \tag{2.14}$$

Eq. (2.11) or (2.14) is a vector Fredholm integral equation of the second kind for the electric field $\boldsymbol{E}$. The kernel $\mathfrak{G}$ and inhomogeneous term $\boldsymbol{E}_n$ depend only on the normal conductivity structure. The domain of integration is the anomalous domain. To determine the kernel $\mathfrak{G}$ replace first the conductivity within the anomalous domain by its normal values. Then place at each point of the domain two mutually perpendicular horizontal dipoles and one vertical dipole and calculate the resulting vector fields at each point of this domain. At a first glance the work involved appears to be prohibitive, but it is sharply reduced by the reciprocity (2.13) and the isotropy of the normal conductor in horizontal direction. In particular, only one horizontal dipole is required. Since the kernels are independent of σ_a and $\boldsymbol{E}_n$, the same kernels apply if the conductivity within the anomalous domain is changed and/or the external field is altered (e.g. different polarization).

In the simplest, though physically not very interesting case of a uniform whole space with conductivity σ_0 the tensor elements are simply

$$\begin{aligned} k_0^2 G_{ij}(\boldsymbol{r}_0|\boldsymbol{r}) &= (k_0^2 \delta_{ij} - \partial^2/\partial x_i\, \partial x_j) e^{-k_0 R}/(4\pi R) \\ &= \{(1+u+u^2)\delta_{ij} - (3+3u+u^2)\,(x_i - x_{i0})\,(x_j - x_{j0})/R^2\} e^{-u}/(4\pi R^3) \end{aligned} \tag{2.15}$$

(e.g. Morse and Feshbach, 1953, p. 1781). Here, $R=|\boldsymbol{r}-\boldsymbol{r}_0|$, $k_0^2=i\omega\mu_0\sigma_0$, $u=k_0R$, and δ_{ij} is the Kronecker symbol. For a uniform half-space the elements are given in the appendix. A method for calculating the elements for an arbitrary number of layers is presented in Sec. 3.

The integral equation (2.11) or (2.14) is decomposed into a set of linear equations, which are solved either by iterative techniques or by matrix inversion. Suggestions for the use of either of these techniques are given in Sec. 4. When the electric field within the anomaly is known, a second set of kernels is required, which transform the field via (2.11) or (2.14) into the surface field. The kernels for the magnetic field are obtained by considering the curl of (2.11) or (2.14) with respect to $\boldsymbol{r}_0$.

2.3. The Surface Integral Method (Approach B)

Let the anomalous slab be confined to the depth range $z_1\leq z\leq z_2$. Approach B is to solve within the anomalous slab the inhomogeneous equation

$$\text{curl}\ {}^2\boldsymbol{E}_a(\boldsymbol{r})+k^2(\boldsymbol{r})\,\boldsymbol{E}_a(\boldsymbol{r})=-k_a^2(\boldsymbol{r})\,\boldsymbol{E}_n(\boldsymbol{r}) \tag{2.16}$$

(from (2.3), (2.5), and (2.6)) subject to two homogeneous boundary conditions at $z=z_1$ and $z=z_2$, which involve σ_n for $z<z_1$ and $z>z_2$ respectively, and account for the vanishing anomalous field for $z\to\pm\infty$. When (2.16) is solved by finite differences, the discretization involves also the field values one grid point width above and below the anomalous slab. The surface integral method is simply to express these values by a surface integral in terms of the tangential component of $\boldsymbol{E}_a$ at z_1 and z_2, respectively.

Let V_1 and V_2 be the half-spaces $z<z_1$ and $z>z_2$, respectively, and let S_m, $m=1,2$, be the planes $z=z_m$. Let $\boldsymbol{G}_i^{(m)}(\boldsymbol{r}_0|\boldsymbol{r})$, $\boldsymbol{r}_0\in V_m$, $\boldsymbol{r}\in V_m\cup S_m$, be a solution of

$$\text{curl}\ {}^2\boldsymbol{G}_i^{(V)}(\boldsymbol{r}_0|\boldsymbol{r})+k_n^2(\boldsymbol{r})\boldsymbol{G}_i^{(m)}(\boldsymbol{r}_0|\boldsymbol{r})=\hat{\boldsymbol{x}}_i\delta(\boldsymbol{r}-\boldsymbol{r}_0) \tag{2.17}$$

($i=1,2,3$; $m=1,2$) satisfying for $\boldsymbol{r}\in S_m$ the boundary condition

$$\hat{\boldsymbol{z}}\times\boldsymbol{G}_i^{(m)}(\boldsymbol{r}_0|\boldsymbol{r})=0. \tag{2.18}$$

In V_1 and V_2, $\boldsymbol{E}_a$ is a solution of

$$\text{curl}\ {}^2\boldsymbol{E}_a(\boldsymbol{r})+k_n^2(\boldsymbol{r})\,\boldsymbol{E}_a(\boldsymbol{r})=0. \tag{2.19}$$

Multiply (2.19) by $\boldsymbol{G}_i^{(m)}$, (2.17) by $\boldsymbol{E}_a$, integrate the difference with respect to $\boldsymbol{r}$ over V_m, and obtain on using (2.9), (2.18) and $\boldsymbol{E}_a \to 0$ for $\boldsymbol{r} \to \infty$

$$E_{ai}(\boldsymbol{r}_0) = (-1)^m \int_{S_m} \{\hat{\boldsymbol{z}} \times \boldsymbol{E}_a(\boldsymbol{r})\} \cdot \operatorname{curl} \boldsymbol{G}_i^{(m)}(\boldsymbol{r}_0|\boldsymbol{r})\, dA, \tag{2.20}$$

$r_0 \in V_m$, or in tensor notation

$$\boldsymbol{E}_a(I_0) = (-1)^m \int_{S_m} \operatorname{curl} \mathfrak{G}^{(m)}(\boldsymbol{r}_0|\boldsymbol{r})\, \{\hat{\boldsymbol{z}} \times \boldsymbol{E}_a(\boldsymbol{r})\}\, dA,$$

where $\operatorname{curl} \mathfrak{G}^{(m)} = \sum_i \hat{\boldsymbol{x}}_i \operatorname{curl} \boldsymbol{G}_i^{(m)}$.

This is the required mapping, which admits the representation of the field values outside the anomalous layer in terms of the boundary values of the (continuous) tangential component of $\boldsymbol{E}_a$.

A physical interpretation of Green's vector $\boldsymbol{G}_i^{(m)}(\boldsymbol{r}_0|\boldsymbol{r})$ subject to (2.18) is as follows: Reflect the normal conductivity structure for $z < z_1$ and $z > z_2$ at the planes $z = z_1$ and $z = z_2$ respectively, place a unit dipole in x_i-direction at $r_0 \in V_m$ and an image dipole at $\boldsymbol{r}_0' = \boldsymbol{r}_0 + 2\,(z_m - z_0)\hat{\boldsymbol{z}}$, the moment being the opposite for the two horizontal dipoles and the same for the vertical dipole. Then the tangential component of $\boldsymbol{G}_i^{(m)}$ vanishes at $z = z_m$.

Hence, if V_m is a uniform half-space, $\boldsymbol{G}_i^{(m)}$ is constructed from the whole space formula (2.15). Eq. (2.20) then reads

$$E_{ax}(\boldsymbol{r}_0) = |z_0 - z_m| \int_{S_m} F(R) E_{ax}(\boldsymbol{r}) dA, \tag{2.21a}$$

$$E_{ay}(\boldsymbol{r}_0) = |z_0 - z_m| \int_{S_m} F(R) E_{ay}(\boldsymbol{r}) dA, \tag{2.21b}$$

$$E_{az}(\boldsymbol{r}_0) = (-1)^m \int_{S_m} F(R)\{(x - x_0) E_{ax}(\boldsymbol{r}) + (y - y_0) E_{ay}(\boldsymbol{r})\} dA, \tag{2.21c}$$

where $R = |\boldsymbol{r} - \boldsymbol{r}_0|$, $k_0^2 = i\omega\mu_0\sigma_0$, and

$$F(R) = -\frac{1}{2\pi R} \frac{d}{dR} (e^{-k_0 R}/R) = (1 + k_0 R) e^{-k_0 R}/(2\pi R^3).$$

Eqs. (2.21a–c) contain as important subcase the condition at the air-earth interface ($z_1 = 0$, $k_0 = 0$).

Because of the limited range of the kernels, in applications of the surface integral only a small portion of S_m is considered. For E_{ax} and E_{ay} the contribution of the region nearest to $\boldsymbol{r}_0$ is most important. Assuming E_{ax} and E_{ay} to be constant within a small disc of radius ϱ centered perpendicularly over $\boldsymbol{r}_0$, the weight from (2.21a, b) is simply

$$e^{-k_0\lambda} - (\lambda/\sqrt{\lambda^2 + \varrho^2}) e^{-k_0\sqrt{\lambda^2+\varrho^2}},$$

where $\lambda = |z_m - z_0|$ is the vertical grid point width. Under the same conditions the disc does not contribute to E_{az}.

At the vertical boundaries of the anomalous layer the condition $\boldsymbol{E}_a = 0$ might be a very crude approximation, in particular for a small grid. Here, an impedance boundary condition for the tangential component $\boldsymbol{E}_{at}$ of the anomalous electric field,

$$k\,\boldsymbol{E}_{at} = \hat{\boldsymbol{n}} \times \operatorname{curl} \boldsymbol{E}_a,$$

$\hat{\boldsymbol{n}}$ = outward normal, $k^2(\boldsymbol{r}) = i\omega\mu_0\sigma(\boldsymbol{r})$, performs substantially better (Jones, 1964, p. 325).

3. Computation of Green's Tensor

Consider a normal conductivity structure consisting of a non-conducting air half-space (index 0) and M uniform conducting layers with conductivities σ_m, $m = 1,2, \ldots, M$, all different from zero. Let the interfaces be placed at the depths $h_1 = 0, h_2, \ldots, h_M$. To calculate Green's tensor for approach C, two mutually perpendicular horizontal electric dipoles and one vertical electric dipole of unit moment have to be placed at each point, which will be occupied by the anomalous domain, and the three components of each resulting field have to be determined for each interior point of the domain. Because of the horizontal isotropy, in practice one horizontal dipole is sufficient.

The calculation of dipole source fields within a layered structure is a classical problem (e.g. Sommerfeld, 1935; Wait, 1970). In the applications (e.g. electromagnetic sounding, antenna theory), however, only the position of a dipole *above and on* the structure is of interest. Largely referring to the above studies, only the modifications due to the position of the dipole *within* the structure are stated.

Let the dipole with moment in x_i-direction be placed in the μ-th layer at $\boldsymbol{r}_0$, and let $\boldsymbol{G}_i^m(\boldsymbol{r}_0|\boldsymbol{r})$ be the resulting field in the m-th layer at point $\boldsymbol{r}$. The continuity of the tangential components of the electric and magnetic field at interfaces leads to the conditions

$$\hat{\boldsymbol{z}} \times (\boldsymbol{G}_i^{m-1} - \boldsymbol{G}_i^m) = 0,\ \hat{\boldsymbol{z}} \times \operatorname{curl} (\boldsymbol{G}_i^{m-1} - \boldsymbol{G}_i^m) = 0, \qquad z = h_m,\ m = 1,\ldots,M. \tag{3.1}$$

$\boldsymbol{G}_i$ is represented with the aid of a Hertz vector $\boldsymbol{\pi}_i$:

$$\boldsymbol{G}_i^m(\boldsymbol{r}_0|\boldsymbol{r}) = k_m^2\,\boldsymbol{\pi}_i^m(\boldsymbol{r}) - \operatorname{grad} \operatorname{div} \boldsymbol{\pi}_i^m(\boldsymbol{r}), \tag{3.2}$$

where $k_m^2 = i\omega\mu_0\sigma_m$ and $\boldsymbol{\pi}_i^m$ satisfies

$$\Delta\boldsymbol{\pi}_i^m(\boldsymbol{r}) = k_m^2\,\boldsymbol{\pi}_i^m(\boldsymbol{r}) - \hat{\boldsymbol{x}}_i\,\delta(\boldsymbol{r} - \boldsymbol{r}_0)/k_m^2. \tag{3.3}$$

For the sequel a cylindrical co-ordinate system (r,ϕ,z) is adopted and the dipole is placed at $r=0$, $z=z_0$. The vertical and horizontal dipole require different treatment.

α) *Vertical Dipole*

$\boldsymbol{\pi}_z^m$ has a vertical component only,

$$\boldsymbol{\pi}_z^m(\boldsymbol{r}) = \pi_{zz}^m(\boldsymbol{r})\hat{\boldsymbol{z}}, \tag{3.4}$$

where π_{zz}^m satisfies

$$\Delta\pi_{zz}^m(\boldsymbol{r}) = k_m^2\pi_{zz}^m(\boldsymbol{r}) - \delta(\boldsymbol{r}-\boldsymbol{r}_0)/k_m^2. \tag{3.5}$$

Eq. (3.1) implies the boundary conditions

$$\sigma_{m-1}\pi_{zz}^{m-1} - \sigma_m\pi_{zz}^m = 0,\ \frac{\partial}{\partial z}(\pi_{zz}^{m-1} - \pi_{zz}^m) = 0,\ z = h_m. \tag{3.6}$$

The general solution of circular symmetry of the homogeneous version of (3.5) can be built up from terms of the form

$$f_m^{\pm}(z)J_0(sr),\ \text{where } f_m^{\pm} = e^{\pm\alpha_m(z-h_m)},\ \alpha_m^2 = s^2 + k_m^2,\ m = 0,\ldots,M \tag{3.7a-c}$$

with $h_0=0$; s is the constant of separation and J_0 the zero order Bessel function of the first kind. The plus and minus sign denote upward and downward travelling waves, respectively. The solution of (3.5) for a uniform whole-space with $\sigma=\sigma_\mu$ is

$$\frac{e^{-k_\mu R}}{4\pi k_\mu^2 R} = \frac{1}{4\pi k_\mu^2}\int_0^\infty \frac{s}{\alpha_\mu} e^{-\alpha_\mu|z-z_0|}J_0(sr)ds,\ R = |\boldsymbol{r}-\boldsymbol{r}_0|. \tag{3.8}$$

Now let for $0\leq m\leq M$

$$\pi_{zz}^m = \int_0^\infty (P_m^+ + P_m^-)J_0\,ds,\ \text{where } P_m^{\pm} = \begin{cases}\gamma_0 A_m^{\pm} f_m^{\pm}, & z\leq z_0\\ \gamma_M B_m^{\pm} f_m^{\pm}, & z\geq z_0\end{cases}. \tag{3.9}$$

$A_m^{\pm}$, $B_m^{\pm}$, γ_0 and γ_M are also functions of s; γ_0 and γ_M being so adjusted that $A_0^+ = B_M^- = 1$. The absence of downgoing waves for $z\leq 0$ and upgoing waves for $z\geq z_0$, if z_0 is in the M-th layer, yields $A_0^- = B_M^+ = 0$.

Starting with $A_0^+ = 1$, $A_0^- = 0$, the boundary conditions imply for $1 \leq m \leq \mu$ the recurrence relations

$$\begin{aligned} A_m^\pm = &\left(\frac{\sigma_{m-1}}{\sigma_m} \pm \frac{\alpha_{m-1}}{\alpha_m}\right) g_{m-1}^+ A_{m-1}^+ \\ &+ \left(\frac{\sigma_{m-1}}{\sigma_m} \mp \frac{\alpha_{m-1}}{\alpha_m}\right) g_{m-1}^- A_{m-1}^- , \end{aligned} \tag{3.10}$$

where

$$g_m^\pm = \frac{1}{2} e^{\pm a_m (h_{m+1} - h_m)}, \quad m = 0, \ldots, M-1. \tag{3.11}$$

Similarly starting with $B_M^+ = 0$, $B_M^- = 1$, Eq. (3.6) yields for $M-1 \geq m \geq \mu$ the backward recurrence relations

$$B_m^\pm = \left(\frac{\sigma_{m+1}}{\sigma_m} \pm \frac{\alpha_{m+1}}{\alpha_m}\right) g_m^\mp B_{m+1}^+ + \left(\frac{\sigma_{m+1}}{\sigma_m} \mp \frac{\alpha_{m+1}}{\alpha_m}\right) g_m^\mp B_{m+1}^- . \tag{3.12}$$

In the case $\mu = M$ no recurrence is required for $B_m^\pm$. Having computed $A_\mu^\pm$ and $B_\mu^\pm$ via (3.10) and (3.12), γ_0 and γ_M are determined from

$$(\gamma_0 A_\mu^- - \gamma_M B_\mu^-) f_\mu^- (z_0) = (\gamma_M B_\mu^+ - \gamma_0 A_\mu^+) f_\mu^+ (z_0) = \frac{-s}{4\pi\alpha_\mu k_\mu^2} . \tag{3.13}$$

The first equality results from (3.9) for $z = z_0$, the second from the fact that the difference in the upgoing (downgoing) waves for $z > z_0$ and $z < z_0$ is due to the primary excitation, given by (3.8). Hence,

$$\begin{aligned} \gamma_0 &= \frac{s}{4\pi\alpha_\mu k_\mu^2} \cdot \frac{B_\mu^- f_\mu^- + B_\mu^+ f_\mu^+}{\Delta (A,B)} , \\ \gamma_M &= \frac{s}{4\pi\alpha_\mu k_\mu^2} \cdot \frac{A_\mu^- f_\mu^- + A_\mu^+ f_\mu^+}{\Delta (A,B)} , \end{aligned} \tag{3.14}$$

where $f_\mu^\pm = f_\mu^\pm (z_0)$ and

$$\Delta(A,B) = A_\mu^+ B_\mu^- - A_\mu^- B_\mu^+ . \tag{3.15}$$

When π_{zz}^m is determined, the tensor elements G_{zx}, G_{zy}, G_{zz} are calculated via (3.4) from (3.2). The field in $z \leq 0$ is simply

$$\boldsymbol{G}_z^0 = -\operatorname{grad} \left(\int_0^\infty \gamma_0 e^{sz} J_0 s ds \right) \tag{3.16}$$

β) Horizontal Dipole

Let the dipole be directed along the x-axis. The Hertz vector has two components now:

$$\boldsymbol{\pi}_x^m(\boldsymbol{r}) = \pi_{xx}^m(\boldsymbol{r})\,\hat{\boldsymbol{x}} + \pi_{xz}^m(\boldsymbol{r})\,\hat{\boldsymbol{z}}. \tag{3.17}$$

From (3.3) follow the differential equations

$$\Delta\,\pi_{xx}^m = k_m^2\,\pi_{xx}^m - \delta(\boldsymbol{r}-\boldsymbol{r}_0)/k_m^2, \quad \Delta\,\pi_{xz}^m = k_m^2\,\pi_{xz}^m. \tag{3.18a,b}$$

Eq. (3.1) yields four boundary conditions at $z=h_m$:

$$\sigma_{m-1}\,\pi_{xx}^{m-1} - \sigma_m\,\pi_{xx}^m = 0, \quad \frac{\partial}{\partial z}(\sigma_{m-1}\,\pi_{xx}^{m-1} - \sigma_m\,\pi_{xx}^m) = 0, \tag{3.19a,b}$$

$$\sigma_{m-1}\,\pi_{xz}^{m-1} - \sigma_m\,\pi_{xz}^m = 0\,, \ \operatorname{div}(\boldsymbol{\pi}_x^{m-1} - \boldsymbol{\pi}_x^m) = 0\,. \tag{3.19c,d}$$

Condition (3.19d) couples π_{xx} and π_{xz}. — Particular solutions of the homogeneous versions of (3.18a,b) are

$$f_m^{\pm}(z)\,J_n(sr)\cos n\phi \ \text{ and } \ f_m^{\pm}(z)\,J_n(sr)\sin n\phi\,,$$

where J_n is the n-th order Bessel function and $f_m^{\pm}$ is given by (3.7b). Since the excitation is expressed by (3.8), J_0 is appropriate for π_{xx}. Condition (3.19d) then shows that $J_1\cos\phi$ is the correct choice for π_{xz} (ϕ reckoned positive from the x-axis in direction to the y-axis). Let for $0\leq m\leq M$

$$k_m^2\,\pi_{xx}^m = \int_0^\infty (\mathcal{Q}_m^+ + \mathcal{Q}_m^-)J_0\,ds, \text{ where } \mathcal{Q}_m^{\pm} = \begin{cases}\delta_0 C_m^{\pm} f_m^{\pm}, & z\leq z_0\\ \delta_M D_m^{\pm} f_m^{\pm}, & z\geq z_0\end{cases}. \tag{3.20}$$

Then the determination of $C_m^{\pm}$, $D_m^{\pm}$, δ_0, and δ_M is quite similar to that of $A_m^{\pm}$, $B_m^{\pm}$, γ_0, and γ_M, respectively. Thus the boundary conditions (3.19a,b) yield for $1\leq m\leq\mu$ starting with $C_0^+=1$, $C_0^-=0$:

$$C_m^{\pm} = \left(1 \pm \frac{\alpha_{m-1}}{\alpha_m}\right) g_{m-1}^{+}\,C_{m-1}^{+} + \left(1 \mp \frac{\alpha_{m-1}}{\alpha_m}\right) g_{m-1}^{-}\,C_{m-1}^{-}, \tag{3.21}$$

and starting with $D_M^+=0$, $D_M^-=1$ for $M-1\geq m\geq\mu$:

$$D_m^{\pm} = \left(1 \pm \frac{\alpha_{m+1}}{\alpha_m}\right) g_m^{\mp}\,D_{m+1}^{+} + \left(1 \mp \frac{\alpha_{m+1}}{\alpha_m}\right) g_m^{\mp}\,D_{m+1}^{-}. \tag{3.22}$$

Again, there is no recurrence required for $\mu = M$. The unknowns δ_0 and δ_M are determined similarly to (3.13) and (3.14):

$$\begin{aligned} \delta_0 &= \frac{s}{4\pi\alpha_\mu \Delta(C,D)} (D_\mu^+ f_\mu^+ + D_\mu^- f_\mu^-), \\ \delta_M &= \frac{s}{4\pi\alpha_\mu \Delta(C,D)} (C_\mu^+ f_\mu^+ + C_\mu^- f_\mu^-), \end{aligned} \tag{3.23}$$

where $f_\mu^\pm = f_\mu^\pm(z_0)$, and the Δ-symbol is defined in (3.15). The computation of π_{xz} is slightly more complicated. Let

$$k_m^2 \pi_{xz}^m = \int_0^\infty (R_m^+ + R_m^-) J_1 \cos\phi \, ds,$$

where

$$R_m^\pm = \begin{cases} (\varepsilon_0 E_m^\pm + \delta_0 F_m^\pm) f_m^\pm, & z \leq z_0 \\ (\varepsilon_M G_m^\pm + \delta_M H_m^\pm) f_m^\pm, & z \geq z_0 \end{cases} \tag{3.24}$$

Since at each interface four new coefficients are introduced, whereas there are only the two boundary conditions (3.19c,d), two additional conditions are imposed by equating at each interface the coefficients of ε_0 and δ_0 (or ε_M and δ_M) separately, thus obtaining four pairs of decoupled recurrence relations (using (3.21 and (3.22) to remove $C_{m-1}^\pm$ and $D_m^\pm$):

$$E_m^\pm = \left(1 \pm \frac{\beta_{m-1}}{\beta_m}\right) g_{m-1}^+ E_{m-1}^+ + \left(1 \mp \frac{\beta_{m-1}}{\beta_m}\right) g_{m-1}^- E_{m-1}^-, \tag{3.25}$$

$$\begin{aligned} F_m^\pm = &\left(1 \pm \frac{\beta_{m-1}}{\beta_m}\right) g_{m-1}^+ F_{m-1}^+ + \left(1 \mp \frac{\beta_{m-1}}{\beta_m}\right) g_{m-1}^- F_{m-1}^- \\ &\pm \frac{s}{2\alpha_m} \left(1 - \frac{\sigma_m}{\sigma_{m-1}}\right) (C_m^+ + C_m^-), \end{aligned} \tag{3.26}$$

$$G_m^\pm = \left(1 \pm \frac{\beta_{m+1}}{\beta_m}\right) g_m^\mp G_{m+1}^+ + \left(1 \mp \frac{\beta_{m+1}}{\beta_m}\right) g_m^\mp G_{m+1}^-, \tag{3.27}$$

$$\begin{aligned} H_m^\pm = &\left(1 \pm \frac{\beta_{m+1}}{\beta_m}\right) g_m^\mp H_{m+1}^+ + \left(1 \mp \frac{\beta_{m+1}}{\beta_m}\right) g_m^\mp H_{m+1}^- \\ &\pm \frac{s}{\alpha_m} \left(1 - \frac{\sigma_m}{\sigma_{m+1}}\right) g_m^\mp (D_{m+1}^+ + D_{m+1}^-), \end{aligned} \tag{3.28}$$

where $\beta_m = \alpha_m / \sigma_m$.

To determine ε_0 and ε_M, Eq. (3.24) is considered at $z = z_0$. Since π_{xz} has no singularity, upward and downward travelling waves agree. Hence,

$$\varepsilon_0 E_\mu^\pm + \delta_0 F_\mu^\pm = \varepsilon_M G_\mu^\pm + \delta_M H_\mu^\pm,$$

or

$$\varepsilon_0 = \{\Delta(F, G)\,\delta_0 + \Delta(G, H)\,\delta_M\} / \Delta(G, E), \tag{3.29a}$$

$$\varepsilon_M = \{\Delta(F, E)\,\delta_0 + \Delta(E, H)\,\delta_M\} / \Delta(G, E). \tag{3.29b}$$

So far, the starting values for the recurrence (3.25)—(3.28) have not been specified. Since in the last layer there is no upward travelling wave below the source,

$$G_M^- = 1,\ G_M^+ = H_M^+ = H_M^- = 0 \tag{3.30a}$$

is a correct choice of the initial values of (3.27) and (3.28). For the air layer, a corresponding choice of $E_0^+ = 1$, $E_0^- = F_0^- = F_0^+ = 0$ would be appropriate, if the air had non-zero conductivity. In the case of $\sigma_0 = 0$, (3.25) and (3.26) break down. As a remede recurrence has to start at $m = 2$ and the coefficients for $m = 1$ must be specified. Assume for the moment that the air half-space is slightly conducting, i.e. $k_0^2 \neq 0$. Whereas $\boldsymbol{\pi}_x$ is only an auxiliary function, the quantities $k_0^2 \boldsymbol{\pi}_x^0$ and $\operatorname{div} \boldsymbol{\pi}_x^0$, entering in (3.2), have a physical meaning and must be finite for $z < 0$. Let

$$k_0^2 \pi^0{}_{xz} = \int_0^\infty \tilde{\varepsilon}_0\, e^{sz} J_1 \cos\phi\, ds.$$

Then $\operatorname{div} \pi_x^0$ is finite if $(\tilde{\varepsilon}_0 - \delta_0)/k_0^2$ is finite for $\sigma_0 \to 0$. Hence, $\tilde{\varepsilon}_0 = \delta_0$. Satisfying the boundary condition (3.19c) at $z = 0$ by equating the coefficients of ε_0 and δ_0 separately, yields $E_1^- + E_1^+ = 0$, $F_1^- + F_1^+ = 1$. Specifying ε_0 as the amplitude of the upward propagating wave in the first layer, the final starting values

$$E_1^- = -1,\ E_1^+ = 1,\ F_1^- = 1,\ F_1^+ = 0 \tag{3.30b}$$

are obtained. This completes the treatment of the horizontal dipole.

Now, on using (3.2), (3.9), (3.20), and (3.24) all tensor elements can be given explicitly. Let

$$U_1 = \int_0^\infty \{Q_m^+ + Q_m^-\} J_0\, ds + \frac{1}{k_m^2 r} \int_0^\infty \{s(Q_m^+ + Q_m^-) - \alpha_m(R_m^+ - R_m^-)\} J_1\, ds,$$

$$U_2 = -\frac{1}{k_m^2} \int_0^\infty \{s(Q_m^+ + Q_m^-) - \alpha_m(R_m^+ - R_m^-)\} J_2\, s\, ds,$$

$$U_3 = -\int_0^\infty \{P_m^+ + P_m^-\} J_0\, s^2\, ds,$$

$$U_4 = -\int_0^\infty \{P_m^+ - P_m^-\} J_1\, \alpha_m\, s\, ds,$$

where $U_i = U_i(z_0, z, r)$, $i = 1, \ldots, 4$. Then

$G_{xx}^m = U_1 + U_2 \cos^2\phi$, $G_{xy}^m = G_{yx}^m = U_2 \sin\phi \cos\phi$, $G_{yy}^m = U_1 + U_2 \sin^2\phi$

$G_{zx}^m = U_4 \cos\phi$, $G_{zy}^m = U_4 \sin\phi$, $G_{zz}^m = U_3$.

The missing elements G_{xz}^m, G_{yz}^m can also be expressed by Q and R terms, or simpler on using the reciprocity (2.13), as

$G_{xz}^m = -U_4(z, z_0, r) \cos\phi$, $G_{yz}^m = -U_4(z, z_0, r) \sin\phi$.

The sign is reversed, since the interchange of source and receiver changes ϕ by π. The nine elements of $\mathfrak{G}$ can be expressed in terms of the four auxiliary functions U_1 to U_4. For $i = 1, 2, 3$ reciprocity requires $U_i(z_0, z, r) = U_i(z, z_0, r)$. Hence, these functions have to be determined for $z \leq z_0$ only.

The tensor elements which transform the electric field within the anomalous domain into the surface field, become particularly simple. Eqs. (3.19 d) and (3.20) yield

$$k_1^2 \operatorname{div} \boldsymbol{\pi}_x^0 = \int_0^\infty \{2\, \alpha_1\, \varepsilon_0 - (\alpha_1 + s)\delta_0\}\, e^{sz} J_1 \cos\phi\, ds\,. \tag{3.31}$$

Hence, defining

$$V_1 = \int_0^\infty \delta_0 J_0\, ds + \frac{1}{k_1^2 r} \int_0^\infty \{(s + \alpha_1)\, \delta_0 - 2\, \alpha_1\, \varepsilon_0\} J_1\, ds,$$

$$V_2 = -\frac{1}{k_1^2} \int_0^\infty \{(s + \alpha_1)\, \delta_0 - 2\, \alpha_1 \varepsilon_0\} J_2\, s\, ds,$$

$$V_3 = -\int_0^\infty \gamma_0 J_0\, s^2\, ds, \quad V_4 = \int_0^\infty \gamma_0 J_1\, s^2\, ds,$$

$$V_5 = \int_0^\infty \delta_0 J_1\, ds + \frac{1}{k_1^2} \int_0^\infty \{(s + \alpha_1)\, \delta_0 - 2\, \alpha_1\, \varepsilon_0\} J_1\, s\, ds,$$

where $V_i = V_i(z_0, r)$, Eq. (3.2) yields as tensor elements for $z = -0$:

$G_{xx}^0 = V_1 + V_2 \cos^2\phi$, $G_{xy}^0 = V_2 \sin\phi \cos\phi$, $G_{xz}^0 = V_5 \cos\phi$

$G_{yx}^0 = G_{xy}^0$, $G_{yy}^0 = V_1 + V_2 \sin^2\phi$, $G_{yz}^0 = V_5 \sin\phi$

$G_{zx}^0 = V_4 \cos\phi$, $G_{zy}^0 = V_4 \sin\phi$, $G_{zz}^0 = V_3$.

In $z \leq 0$, the electric field of a dipole in x-direction (say),

$$\boldsymbol{G}_x^0 = \int_0^\infty \delta_0(\hat{\boldsymbol{x}} J_0 + \hat{\boldsymbol{z}} J_1 \cos\phi)\, e^{sz}\, ds - \text{grad div}\, \boldsymbol{\pi}_x^0, \tag{3.32}$$

where $\text{div}\boldsymbol{\pi}_x^0$ is given by (3.31), can be split uniquely into a toroidal part $\boldsymbol{T}$ (purely tangential) and a poloidal part $\boldsymbol{S}$,

$$\boldsymbol{G}_x^0 = \boldsymbol{T} + \boldsymbol{S},\ \boldsymbol{T} = \text{curl}\,(\hat{\boldsymbol{z}}\,\psi_T)\,,\ \boldsymbol{S} = \text{grad}\,\psi_S\,. \tag{3.33}$$

The poloidal part is due to surface charges at $z = 0$. Since the z-component of the first term of (3.32) is poloidal per definition, ψ_S and ψ_T are given by

$$\psi_S = \int_0^\infty \delta_0\, s^{-1} J_1 \cos\phi\, e^{sz}\, ds - \text{div}\,\boldsymbol{\pi}_x^0,\quad \psi_T = \int_0^\infty \delta_0\, s^{-1} J_1 \sin\phi\, e^{sz}\, ds. \tag{3.34}$$

The electric field of a vertical dipole is purely poloidal in $z \leq 0$ (cf. (3.16)). When the kernels for the toroidal part are calculated by (3.33) and (3.34), the electric surface field obtained by (2.14) is easily decomposed into its poloidal and toroidal part. For an elongated anomaly and a toroidal external electric field, the resulting anomalous field is either almost toroidal or poloidal, according whether the external field is parallel or perpendicular to the strike.

In $z \leq 0$ only the toroidal part of the surface electric field gives rise to a magnetic field. Let $\boldsymbol{F}_i^0(\boldsymbol{r}_0|\boldsymbol{r})$, $i = 1, 2$, be the magnetic field at $\boldsymbol{r}$ due to a horizontal dipole in x_i-direction at $\boldsymbol{r}_0$. Then from (2.2)

$$i\omega\mu_0\, \boldsymbol{F}_i^0(\boldsymbol{r}_0|\boldsymbol{r}) = -\,\text{curl}\, \boldsymbol{G}_i^0(\boldsymbol{r}_0|\boldsymbol{r})\,,\ i = 1,2\,.$$

Defining

$$i\omega\mu_0\, W_1 = \int_0^\infty \delta_0 \left(\frac{1}{sr} J_1 - J_0\right) s\, ds,\ i\omega\mu_0\, W_2 = \int_0^\infty \delta_0 J_2\, s\, ds,$$

$$i\omega\mu_0\, W_3 = -\int \delta_0 J_1\, s\, ds,$$

the magnetic field kernels are

$$F_{xx}^0 = -\,W_2 \sin\phi\cos\phi,\quad F_{xy}^0 = W_1 + W_2\cos^2\phi,\ F_{xz}^0 = W_3 \sin\phi,$$
$$F_{yx}^0 = -\,W_1 - W_2 \sin^2\phi,\ F_{yy}^0 = W_2 \sin\phi\cos\phi,\quad F_{yz}^0 = -\,W_3\cos\phi.$$

Hence, the determination of the electric and magnetic surface field requires the tabulation of eight additional functions (V_1 to V_5 and W_1 to W_3), all functions of z_0 and r. The range of r depends on the surface domain, where the anomalous field is to be evaluated.

4. *Numerical Considerations*

The integral equation (2.11) or (2.14) is solved by the simple approximate approach of Hohmann (1971). It consists in decomposing the anomalous domain into a set of equal rectangular cells, assuming a constant electric field within each cell. For N cells results a linear system of $3N$ equations and unknowns. The coefficients are essentially the tensor kernels integrated with respect to source coordinates (Eq. (2.14)) or observer coordinates (Eq. (2.11)) over a cell. Care must be exercised in evaluating the contribution of the singular cell and of its neighbourhood. In general, the most important contribution arises from the primary excitation in direction of its moment. Let the dimensions of a cell be λ_x, λ_y, λ_z, and let

$$G^p_{xx} = (k^2 - \partial^2/\partial x^2)\, e^{-kR}/(4\pi k^2 R)$$

be the excitation in x-direction. For an approximate evaluation, the singular cell C_S is replaced in the first term by a sphere of the same volume and in the second term by a circular cylinder with axis in x-direction, length λ_x and cross-section $\lambda_y \cdot \lambda_z$. It results

$$k^2 \int_{C_S} G^p_{xx}\, d\tau = e^{-kR1} - (R_1/R_2)\, e^{-kR2} - (1 + kR_3)\, e^{-kR3} + 1,$$

where $R_1 = \lambda_x/2$, $R_2^2 = \lambda_x^2/4 + \lambda_y \lambda_z/\pi$, $R_3^3 = 3\, \lambda_x \lambda_y \lambda_z/(4\pi)$.

For symmetry reasons, there is no contribution from G^p_{xy} and G^p_{xz}. The integrals over the adjacent cells can be effected in a similar way. In the numerical evaluation of the kernels given in Sec. 3, the integration with respect to z is easily included by adding in the integrand the factor

$$2 \sinh(\alpha_\mu \lambda_z/2)/\alpha_\mu,$$

by which $\exp(\pm \alpha_\mu z_0)$ is multiplied when integrated over the thickness of the cell centered at z_0.

The system of equations is solved either iteratively (e.g. by means of the Gauß-Seidel method) or by matrix inversion. Because of the large storage required, the latter method is attractive only for small anomalous domains. It is of great advantage to exploit all symmetries. For structures with two vertical symmetry planes, the number of unknowns is reduced to almost 25%, and hence, the storage for matrix inversion is only 1/16 of the original storage. For iterative methods, both the computer time for one iteration and the number of iterations is reduced.

The Gauß-Seidel iterative scheme converges only for moderate conductivity contrasts. In numerical experiments it was found that a good convergence can be obtained for conductivity contrasts up to 1:100 only; $\boldsymbol{E}_n$ was used as initial guess for $\boldsymbol{E}$. If for higher contrasts matrix inversion is not possible, the best remede might be to apply the powerful method of shifting the spectrum as described by Hutson *et al.* (1972, 1973).

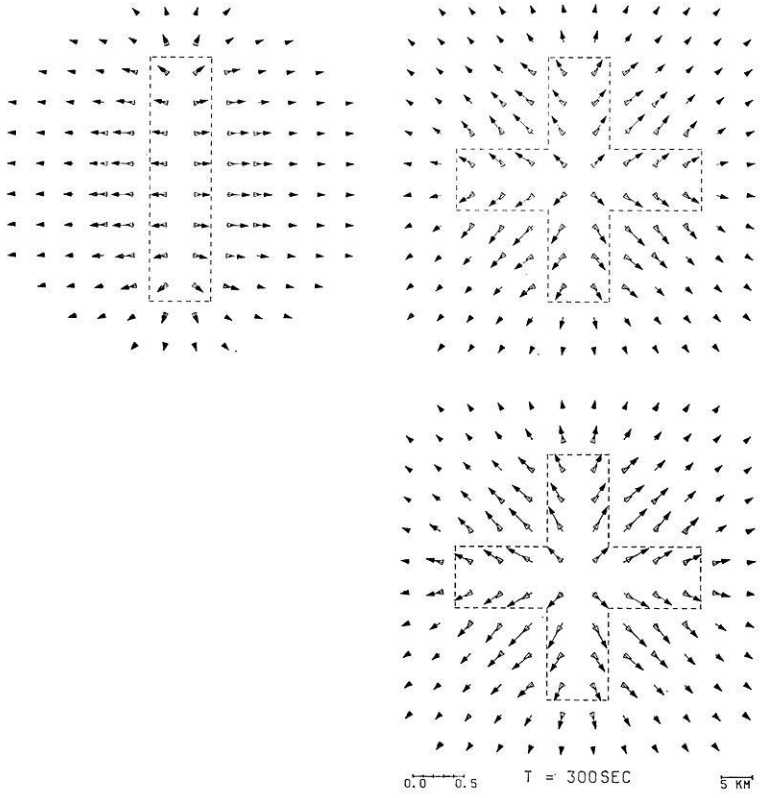

Fig. 2. Induction arrow maps for two different configurations of the anomalous domain (top). Vectorial addition of the arrow of the left structure and of a similar structure rotated through 90° (bottom). Only arrows longer than one half of the length of an arrow head are shown

5. *Results*

The feasibility of the integral equation approach has been tested for simple cases. Some of the results are presented below. A complete and concise presentation of the anomalous field vectors for a three-dimensional model poses a difficult problem. For a quasiuniform external field, 24 displays of a function over a two-dimensional array are required to give a complete description of the in-phase and out-of-phase part of the electric and magnetic field vector for the two mutually perpendicular polarizations of the external field. Four of these displays (in-phase and out-of-phase part of H_z for both polarizations) can be combined to yield an induction arrow map. Examples of such maps are shown in the upper half of Fig. 2 for two different configurations of the anomalous domain. The bodies of

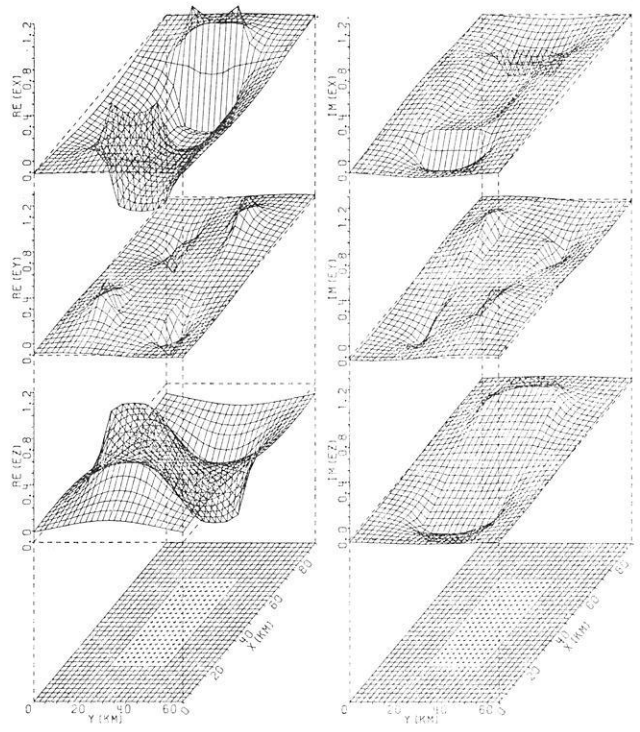

Fig. 3. In-phase and out-of-phase part of the anomalous electric field vector for a uniform external field in x-direction serving as reference field. The associated normal magnetic field points in y-direction. A rectangular anomalous domain, 50 km × 25 km × 10 km of $\varrho = 1\,\Omega$ m, embedded in a uniform half-space with $\varrho = 10\,\Omega$ m just below the surface is chosen. The period of the inducing field is 120 sec

$\varrho = 1$ Ωm are 10 km thick and are placed immediately below the surface of a uniform substratum of $\varrho = 10$ Ωm. In-phase and out-of-phase arrows are marked by black and white heads, respectively. Only arrows longer than one half of the arrow head are shown. It has been proved by Siebert (1971) that the induction arrows for a complex structure, consisting of two elongated, mutually perpendicular anomalies can be obtained approximately by vectorial superposition of the individual arrows. Along this line, the lower map of Fig. 2 has been obtained by adding to the arrows of the left map the arrows of the same structure, rotated through 90°. Since mutual induction is neglected, the induction effect is slightly overestimated.

The complete set of 24 displays for a different high conducting intrusion is illustrated in Figs. 3–6. The plots are thought to provide a qualitative idea of the fields, although quantitative results can be extracted by a some-

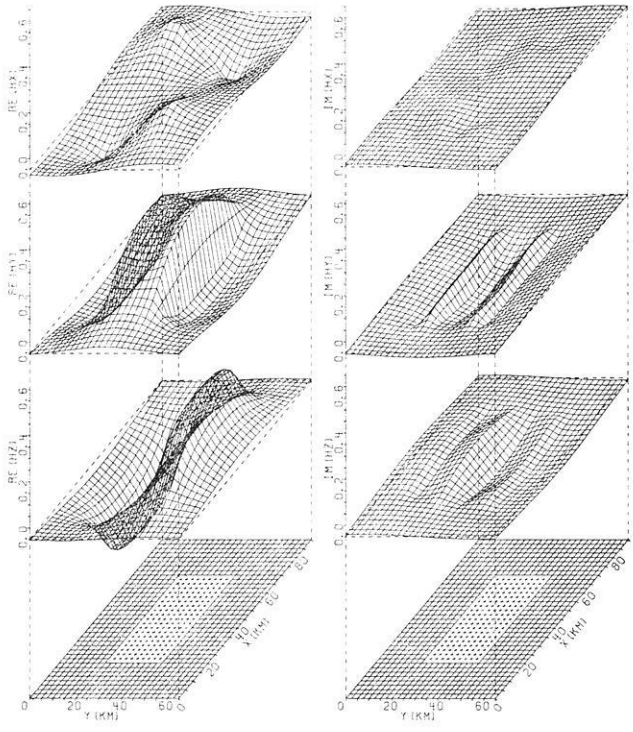

Fig. 4. The anomalous magnetic field of the model described in the caption to Fig. 3. The normal magnetic field serves as reference field

what awkward procedure. The disturbing body is decomposed into cubes with 5 km edges. There are 10, 5, and 2 cubes in x, y, z-direction, respectively. The complete surface field has been evaluated on a 18×13 grid. On a UNIVAC 1108 computer the determination of all kernels took 70 sec, the solution of the integral equation and the evaluation of the surface field required additional 50 sec for each polarization, the Gauß-Seidel iterative scheme being convergent after 10 iterations.

In all subsequent figures, only the anomalous fields are shown. The modulus of the corresponding normal field serves as reference. Fig. 3 presents the electric field for a uniform external electric field in x-direction. The associated normal magnetic field points in y-direction. Within the good conductor, the E_x-component breaks down. It exhibits a discontinuity at the front and rear surface since the normal component of the current density is continuous there. The E_y-component differs appreciably from zero only near the corners. The signs are easily understood using the idea of the electric currents being sucked into the good conductor. The

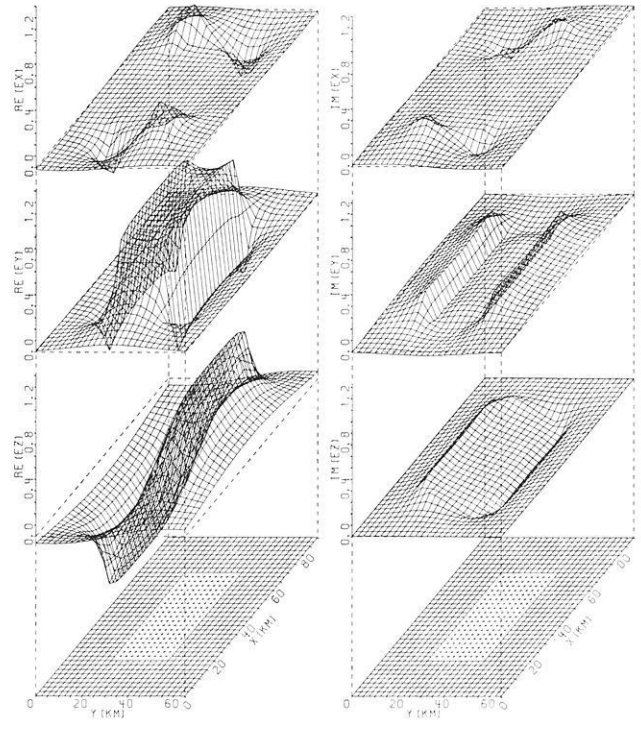

Fig. 5. In-phase and out-of-phase part of the anomalous electric field vector for a uniform external field in -y-direction associated with a normal magnetic field in x-direction. The same anomalous domain and period as in Fig. 3

magnitude of the E_z-component is of the order of E_x. Its origin are surface charges: negative charges at the front bending the current lines towards the surface and positive charges at the rear reflecting the lines from the surface. Fig. 4 shows the corresponding magnetic field. The signs are understood using the idea of magnetic field lines expelled from the good conductor.

Figs. 5 and 6 display the electric and magnetic field for an external magnetic field in x-direction associated with an electric field in -y-direction. With the present choice of the dimensions of the disturbing body, this polarization resembles the two-dimensional H-polarization, i.e. the anomalous magnetic field vanishes if the anomaly is extended to infinity at both ends. In the same limit the former polarization degenerates into the E-polarization case.

After decomposing the kernels $\boldsymbol{G}_{\mathrm{x}}^0$ and $\boldsymbol{G}_{\mathrm{y}}^0$ according to (3.33) and (3.34), the poloidal and toroidal part of the electric surface field can be obtained

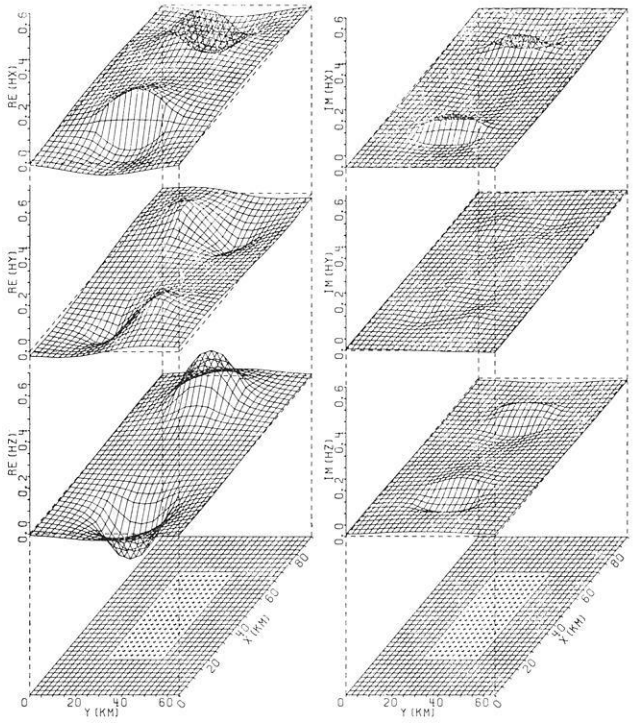

Fig. 6. The anomalous magnetic field vector of the model of Fig. 5

separately. For the E_x and E_y component of Fig. 3 this is done in Figs. 7a and 7b.

Finally, the transition from three to two dimensions has been investigated for a particular model. Fig. 8 illustrates that on a central profile a two-dimensional description is adequate if the length of the disturbing body exceeds three times its width.

6. Conclusion

The integral equation technique based on Green's tensor turns out to be a useful tool in treating three-dimensional induction problems.

It is suitable for small anomalous domains, and here it is of particular advantage if the anomalous field is required for a set of different conductivities within the anomalous domain and/or different external fields, for the time consuming computation of the pertinent kernels has to be carried out once only. Work is still necessary to develop effective iterative methods if the conductivity contrast is large ($>100:1$). For large anomalous domains, a finite difference technique combined with a surface integral boundary condition appears to be the most promising approach.

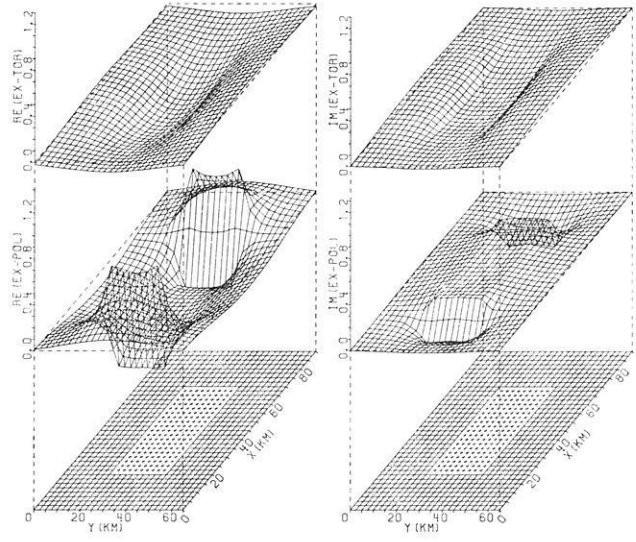

Fig. 7a. Toroidal and poloidal part of the E_x-component of Fig. 3

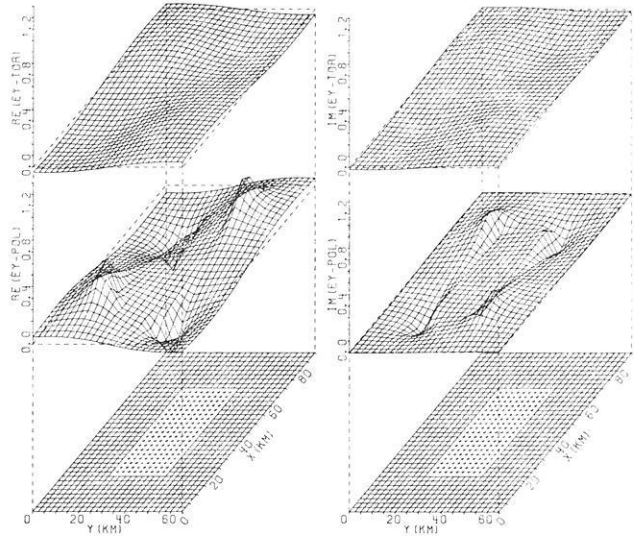

Fig. 7b. Toroidal and anomalous part of the E_y-component of Fig. 3

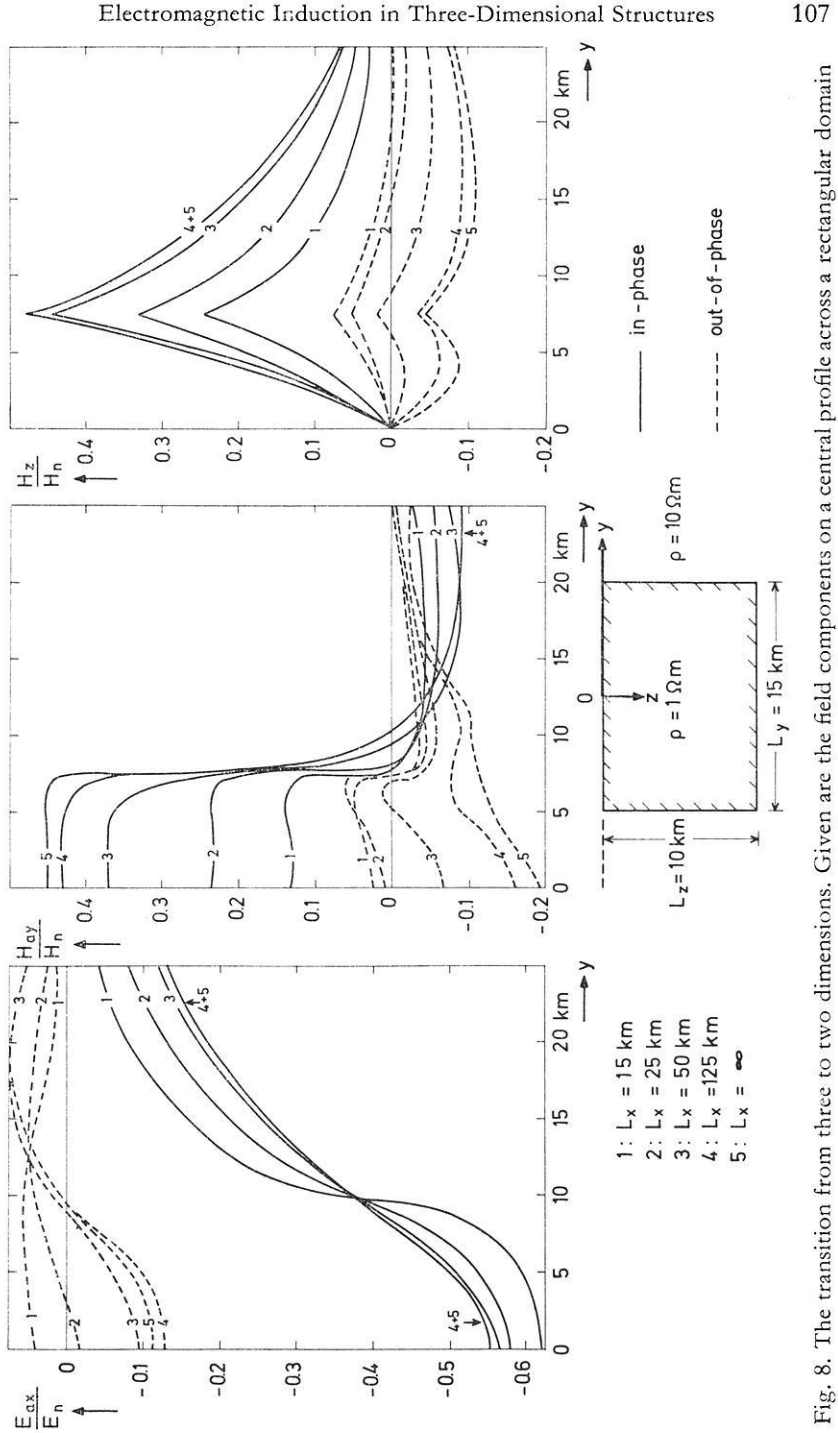

Fig. 8. The transition from three to two dimensions. Given are the field components on a central profile across a rectangular domain with dimensions L_x, L_y, L_z

Appendix

The Tensor Elements for a Uniform Half-Space

For a uniform half-space with $\sigma_n(z) = \sigma_0$ these elements have already been given by Raiche (1974) in terms of integrals. However, all integrations can be carried out explicitly. Using source coordinates x_0, y_0, z_0 and the abbreviations.

$$R_\pm^2 = (x - x_0)^2 + (y - y_0)^2 + (z \pm z_0)^2,$$

$$g_\pm = \exp(-k_0 R_\pm)/(4\pi R_\pm), \quad \alpha_\pm = g_- \pm g_+, \quad k_0^2 = i\omega\mu_0\sigma_0,$$

$$\beta = \alpha_- - (\partial/\partial z)\left\{I_0\left(\frac{1}{2}k_0[R_+ - z - z_0]\right) \cdot K_0\left(\frac{1}{2}k_0[R_+ + z + z_0]\right)\right\}/(2\pi),$$

where I_0 and K_0 are modified Bessel functions of order zero, first and second kind, it results for z, $z_0 > 0$

$$k_0^2 G_{xx} = (k_0^2 - \partial^2/\partial x^2)\beta + (\partial^2/\partial z^2)(\alpha_+ - \beta),$$
$$k_0^2 G_{xy} = k_0^2 G_{yx} = -(\partial^2/\partial x\, \partial y)\beta,$$
$$k_0^2 G_{xz} = -(\partial^2/\partial x\, \partial z)\alpha_+,$$
$$k_0^2 G_{yy} = (k_0^2 - \partial^2/\partial y^2)\beta + (\partial^2/\partial z^2)(\alpha_+ - \beta),$$
$$k_0^2 G_{yz} = -(\partial^2/\partial y \partial z)\alpha_+,$$
$$k_0^2 G_{zx} = -(\partial^2/\partial z \partial x)\alpha_-,$$
$$k_0^2 G_{zy} = -(\partial^2/\partial z \partial y)\alpha_-,$$
$$k_0^2 G_{zz} = (k_0^2 - \partial^2/\partial z^2)\alpha_-.$$

The vertical components G_{xz}, G_{yz}, G_{zz}, vanishing for $z \to +0$, tend for $z \to -0$ to the limiting values

$$k_0^2 G_{xz} = -(\partial^2/\partial x\, \partial z_0)\gamma, \quad k_0^2 G_{yz} = -(\partial^2/\partial y \partial z_0)\gamma,$$
$$k_0^2 G_{zz} = -(\partial^2/\partial z_0^2)\gamma,$$

where

$$\gamma = (\partial/\partial z_0)\left\{I_0\left(\frac{1}{2}k_0[R_0 - z_0]\right) \cdot K_0\left(\frac{1}{2}k_0[R_0 + z_0]\right)\right\}/(2\pi),$$

$$R_0^2 = (x - x_0)^2 + (y - y_0)^2 + z_0^2.$$

Since in applications an integration over the source or observer coordinates (Eqs. (2.14) and (2.11), respectively) is involved, most of the above differentiations need not to be carried out. (Use $\partial/\partial x = -\partial/\partial x_0$, $\partial/\partial y = -\partial/\partial y_0$, and e.g. $\partial\alpha_-/\partial z = -\partial\alpha_+/\partial z_0$, $\partial\alpha_+/\partial z = -\partial\alpha_-/\partial z_0$.)

References

Hohmann, G.W.: Electromagnetic scattering by conductors in the earth near a line source of current, Geophysics *36*, 101–131, 1971

Hutson, V.C.L., Kendall, P.C., Malin, S.R.C.: Computation of the solution of geomagnetic induction problems: a general method, with applications. Geophys. J. *28*, 489–498, 1972

Hutson, V.C.L., Kendall, P.C., Malin, S.R.C.: The modelling of oceans by spherical caps. Geophys. J. *33*, 377–387, 1973

Jones, D.S.: The theory of electromagnetism. Oxford: Pergamon Press 1964

Jones, F.W., Pascoe, L.J.: The perturbation of alternating geomagnetic fields by three-dimensional conductivity inhomogeneities. Geophys. J. *27*, 479–485, 1972

Lines, L.R., Jones, F.W.: The perturbation of alternating geomagnetic fields by three-dimensional island structures. Geophys. J. *32*, 133–154, 1973

Morse, P.M., Feshbach, H.: Methods of theoretical physics. New York: McGraw-Hill 1953

Raiche, A.P.: An integral equation approach to three-dimensional modelling. Geophys. J. *36*, 363–376, 1974

Schmucker, U.: Anomalies of geomagnetic variations in the south-western United States. Bull. Scripps Inst. Ocean. Univ. Calif. *13*, 1970

Schmucker, U.: Neue Rechenmethoden zur Tiefensondierung. In: Protokoll Kolloquium Erdmagn. Tiefensondierung 14.–16. Sept. 1971, Rothenberge/Westf., 1971

Siebert, M.: Zur Deutung von Induktionspfeilen bei schmalen langgestreckten orthogonalen Leitfähigkeitsanomalien. In: Protokoll Kolloquium Erdmagn. Tiefensondierung 14.–16. Sept. 1971, Rothenberge/Westf., 1971

Sommerfeld, A.: Elektromagnetische Schwingungen. In: Frank- v. Mises: Differentialgleichungen der Physik, vol. 2. Braunschweig: Vieweg 1935

Wait, J.R.: Electromagnetic waves in stratified media, 2nd ed. Oxford: Pergamon Press 1970

Weaver, J.T.: The general theory of electromagnetic induction in a conducting half-space. Geophys. J. *22*, 83–100, 1970

Dr. P. Weidelt
Institut für Geophysik der Universität
D-3400 Göttingen
Herzberger Landstraße 180
Federal Republic of Germany